# AGB and related objects at high angular resolution

…

Lopez Bruno
Obs. De la Côte d'Azur, Dpt. Fresnel UMR 6528,
BP 4229 06304 Nice Cedex4, France.

Content : Introduction – A set of questions
The stellar atmosphere ?
The circumstellar medium ?
Perspectives using the interferometry methods

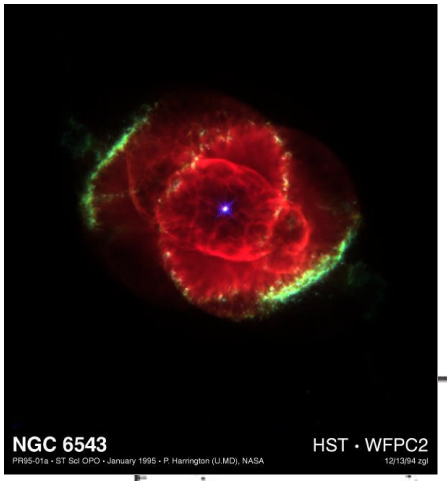
NGC 6543
HST · WFPC2
PR95-01a · ST ScI OPO · January 1995 · P. Harrington (U.MD), NASA
12/13/94 zgl

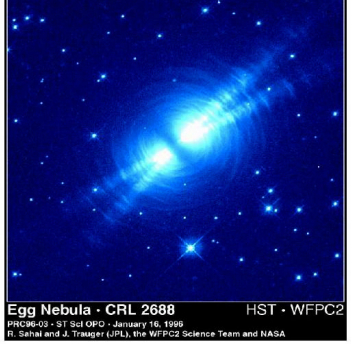
Egg Nebula · CRL 2688
HST · WFPC2
PRC96-03 · ST ScI OPO · January 16, 1996
R. Sahai and J. Trauger (JPL), the WFPC2 Science Team and NASA

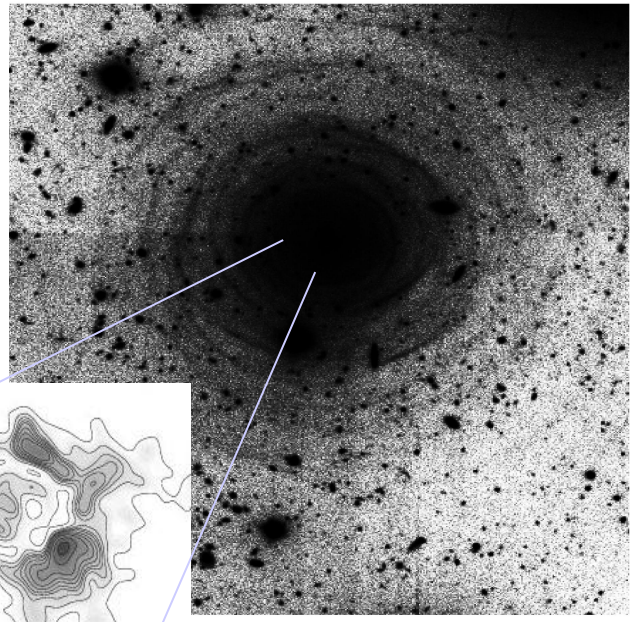



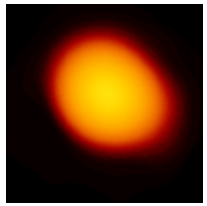

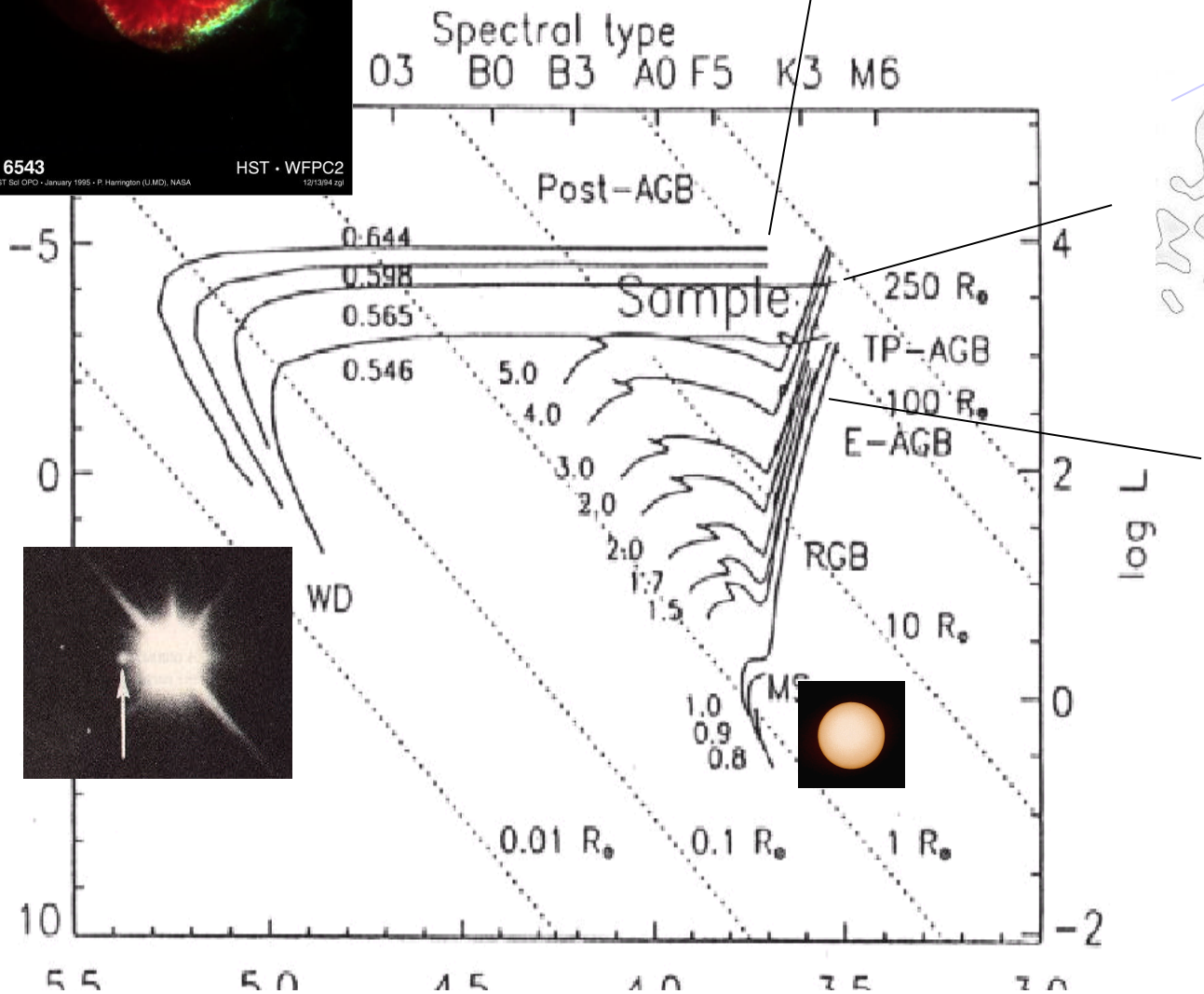
Spectral type
O3 B0 B3 A0 F5 K3 M6
Post-AGB
0.644
0.598
0.565
0.546
Sample
250 R⊙
TP-AGB
100 R⊙
E-AGB
5.0
4.0
3.0
2.0
2.0
1.7
1.5
RGB
10 R⊙
MS
1.0
0.9
0.8
WD
0.01 R⊙
0.1 R⊙
1 R⊙
log L
-5
0
10
4
2
0
-2
5.5
5.0
4.5
4.0
3.5
3.0

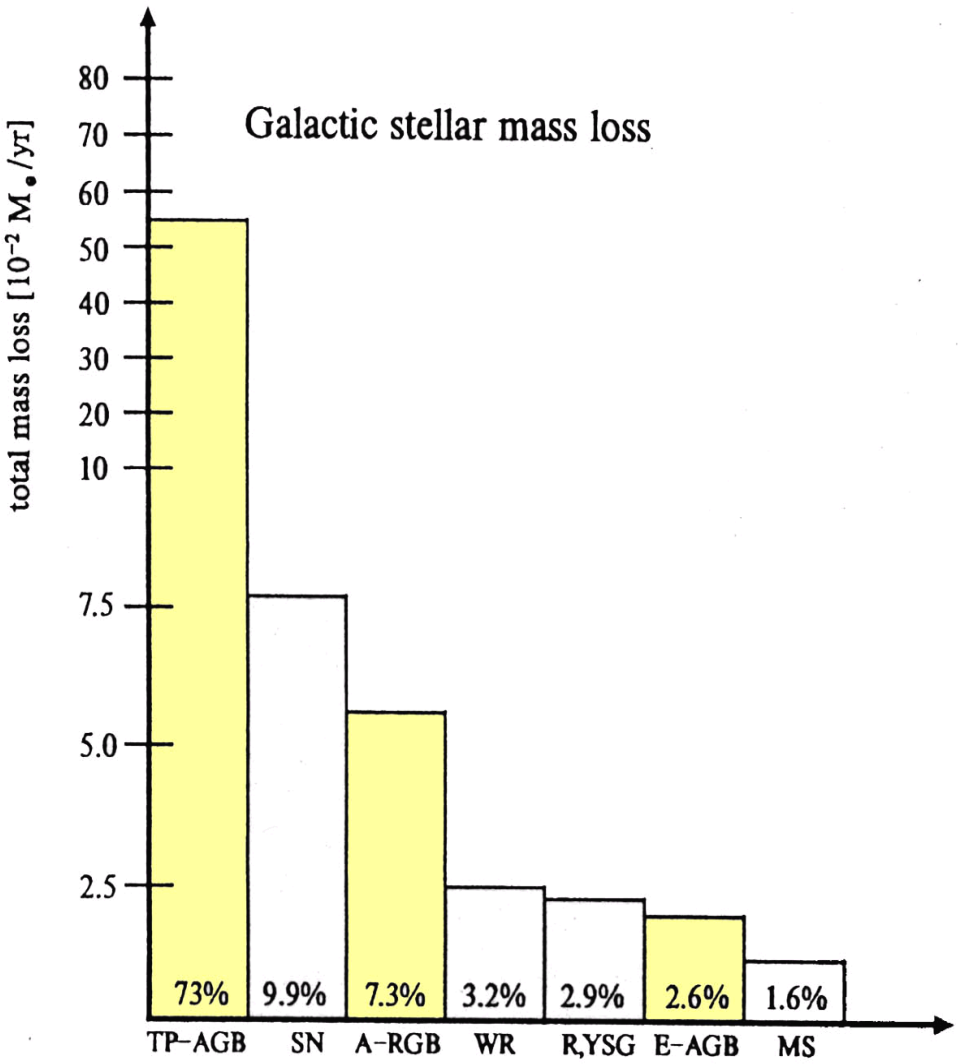


**Fig. 1.** Total galactic mass loss (solar masses per year) of various classes of stellar objects: TP-AGB: tip-AGB objects, SN: supernovae, A-RGB: asymptotic red giant branch, WR-stars, R, YSG: red and yellow supergiants, E-AGB: early AGB objects, MS: main sequence stars. The indicated numbers are collected from the literature and are inferred from a rather inhomogeneous material (Weinzierl 1991). Despite these

Sedlmayr 1994

inclination of the disc, i= 0 °

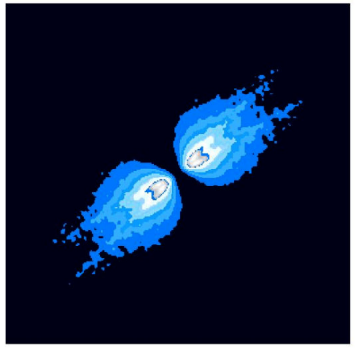

inclination of the disc, i= 5 °

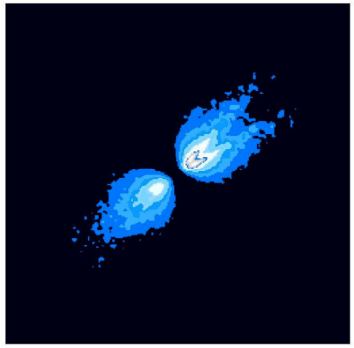

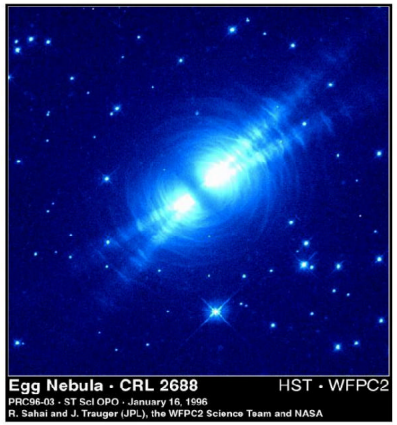


inclination of the disc, i=10 °

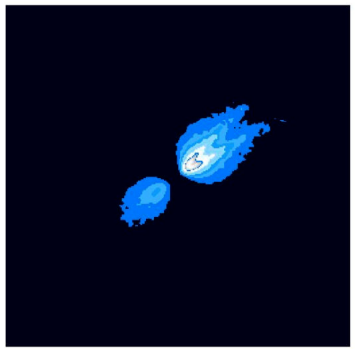

inclination of the disc, i=16 °

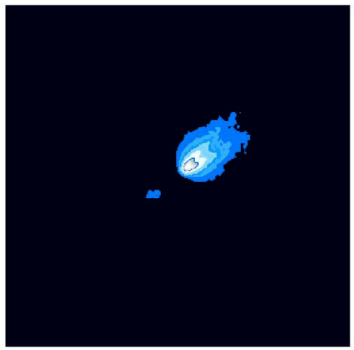

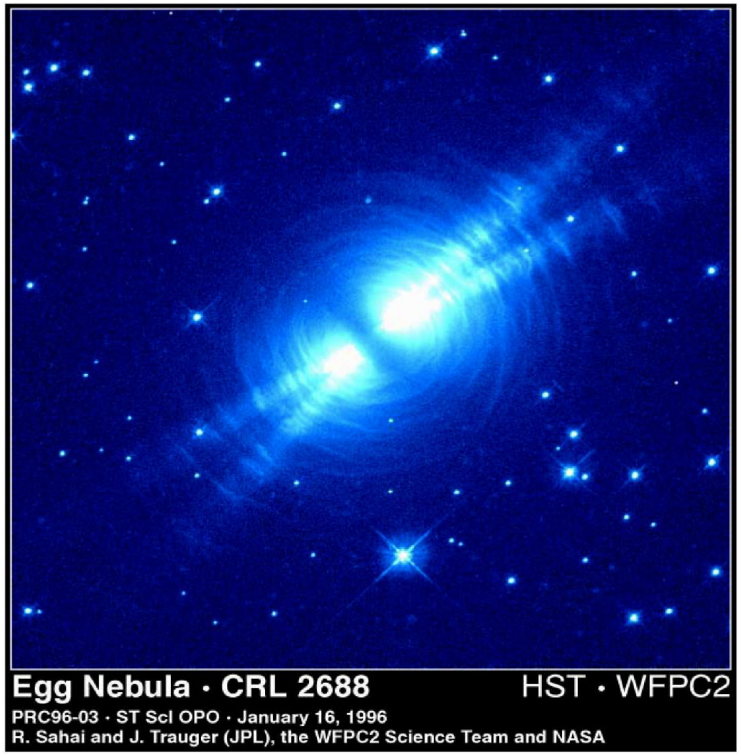


**In about 1000 years …**

**Stingray nebula**

# A set of questions

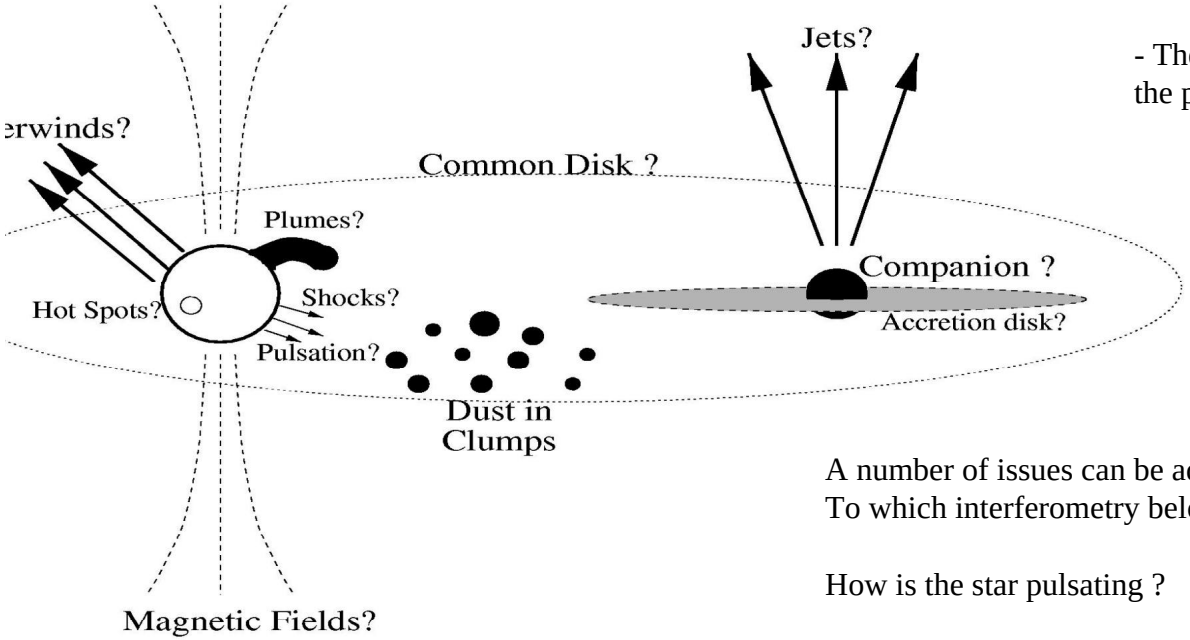


There are two obstacles which prevent to easily observe what causes the mass loss phenomenon (see the Figure 1):

- The mass loss is a combination of several mechanisms; their different contributions are difficult to disentangle

- The wind(s) begin at the stellar surface; ideally the photospheric layers should be angularly resolved.

A number of issues can be addressed to the high angular resolution methods To which interferometry belongs:

How is the star pulsating ?

How are propagating the shock waves ?

When do asymmetries occur during the stellar evolution ?

What may be the causes of departures from spherical symmetry ?

What is observed during the superwind phase ?

Are there observed clumps in the envelopes ?

# The stellar atmosphere ?

Radii and Effective Temperatures for G, K, and M Giants and Supergiants

van Belle et al., AJ 117:521-533, 1999 January

Installations such as the Mark III Interferometer, IOTA (IR Optical Telescope Array), NPOI (Navy Prototype Optical Interferometer), and PTI (the Palomar Testbed Interferometer – 69 evolved stars) have been utilizing their capability to resolve stars in the <20 mas range. These results are significant in that they constitute direct measurements of the parameters of stars that populate the coolest, most luminous portion of the H-R diagram. The release of theHipparcos Catalogue (Perryman et al. 1997) has had the added benefit of allowing many of the observed angular sizes to be interpreted as linear radii.

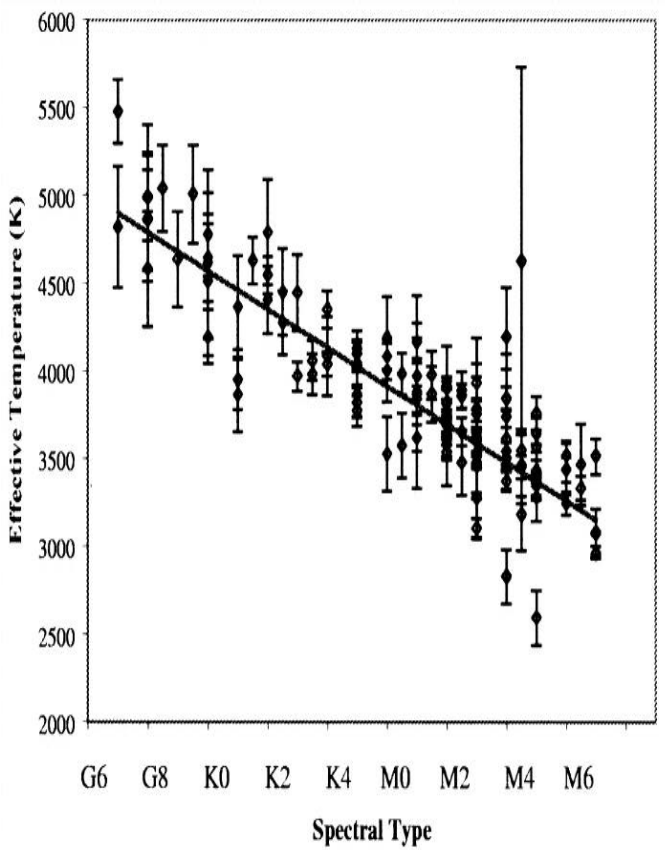


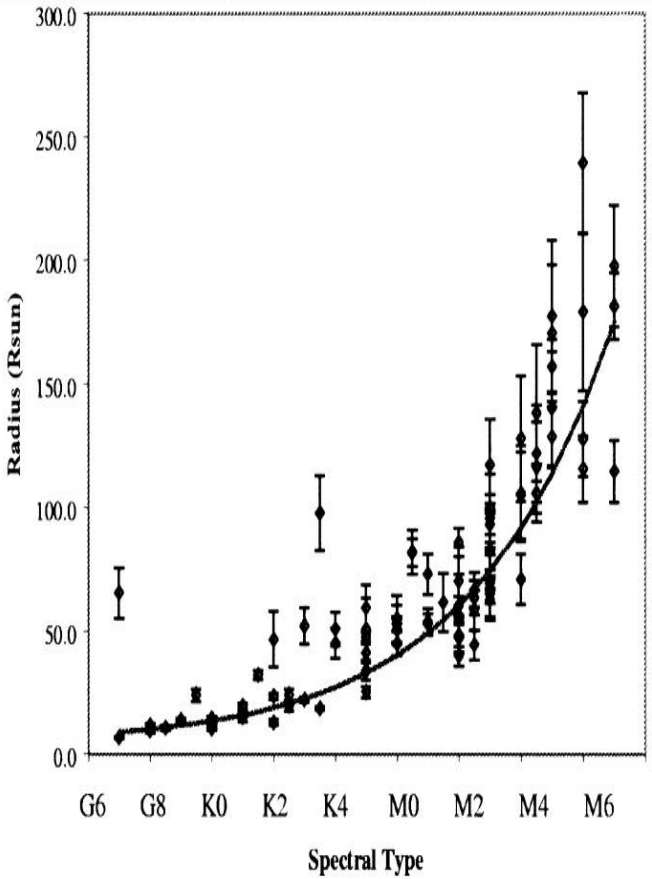

Multi-wavelength bispectrum speckle interferometry of R Leo and comparison with Mira star models

Hofmann et al., 2001, AA 376, 518.

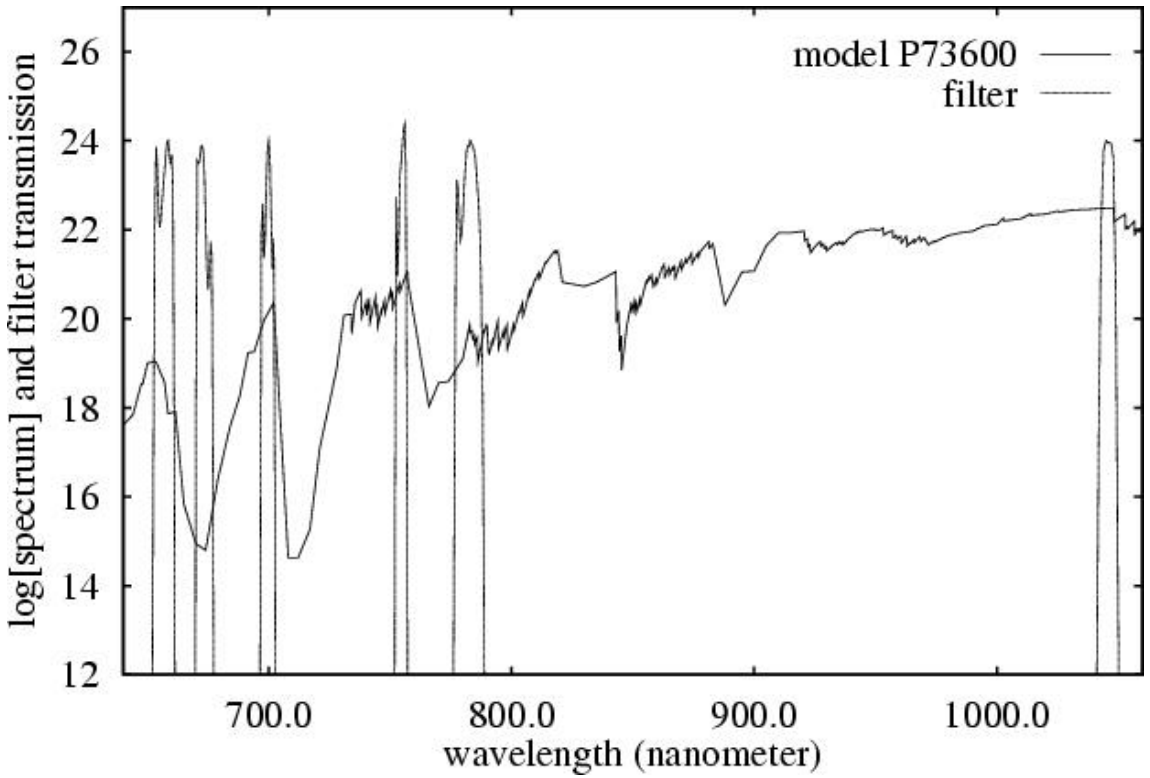

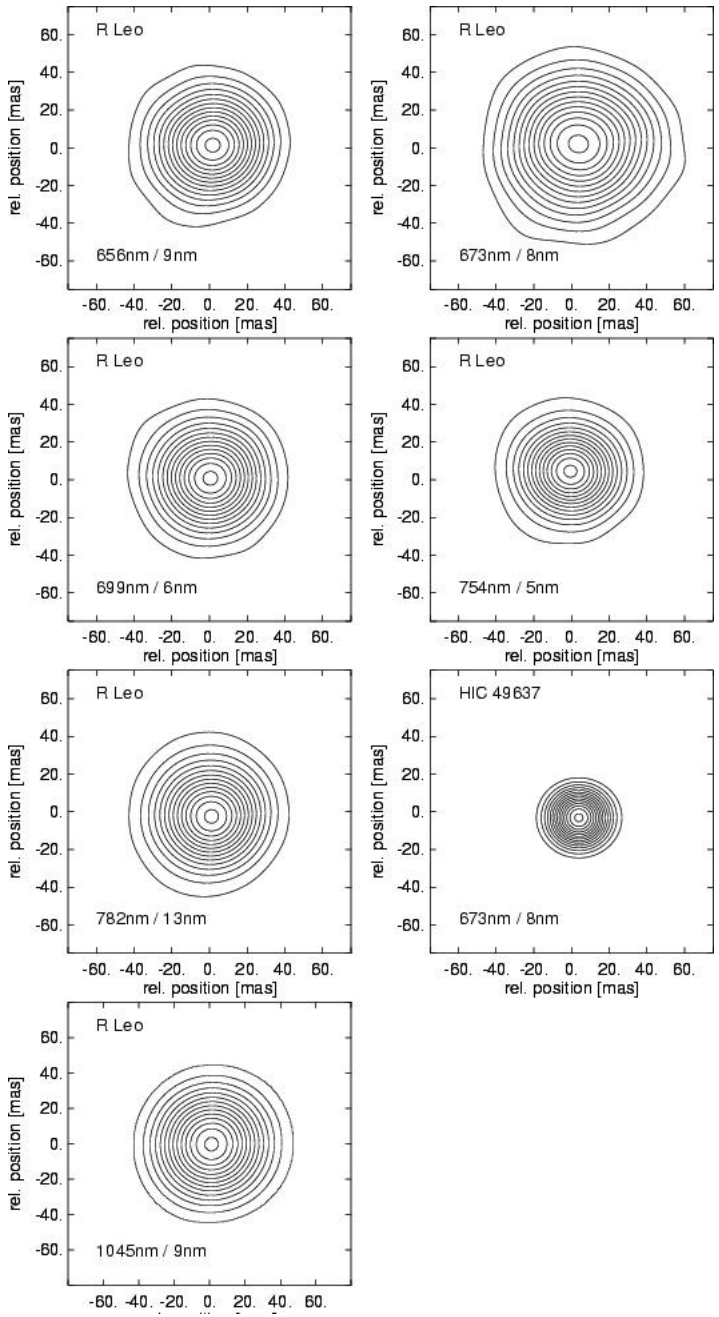


In all six observed wavelength bands the shape of R Leo shows no significant asymmetry..

Monochromatic radii were derived from the observed visibilities by application of model-predicted center-to-limb variations of the intensity. Adopting the HIPPARCOS parallax, a photospheric radius (Rosseland radius) of R Leo of 417 Solar radii is derived indicating pulsation in the first-overtone mode. From JHKL photometry and the angular photospheric radius an effective temperature of about 2590 K at near maximum phase was obtained.

**Table 3.** Linear UD and FDD radii and Gaussian HWHM (in solar radii) based on the HIPPARCOS parallax of R Leo.

| Data set | UD | Gaussian | FDD |
|---|---|---|---|
| 656/10 | $660 \pm 142$ | $415 \pm 89$ | $744 \pm 160$ |
| 673/8 | $823 \pm 177$ | $518 \pm 112$ | $929 \pm 200$ |
| 699/6 | $572 \pm 123$ | $356 \pm 77$ | $642 \pm 138$ |
| 754/6 | $530 \pm 114$ | $332 \pm 72$ | $597 \pm 128$ |
| 781/14 | $599 \pm 129$ | $377 \pm 81$ | $676 \pm 145$ |
| 1045/9 | $413 \pm 97$ | $257 \pm 61$ | $465 \pm 110$ |

Interferometric observations of R Leonis in the K band, First direct detection of the photospheric pulsation and study of the atmospheric intensity distribution

Perrin et al., Astron. Astrophys. 345, 221-232 (1999)

Fit of the 1996 and 1997 data by uniform disk models.
Full circles: 1996 data. Open circles: 1997 data

The linear radius of R Leonis is for the two periods: about 315 and about 345 solar radii.

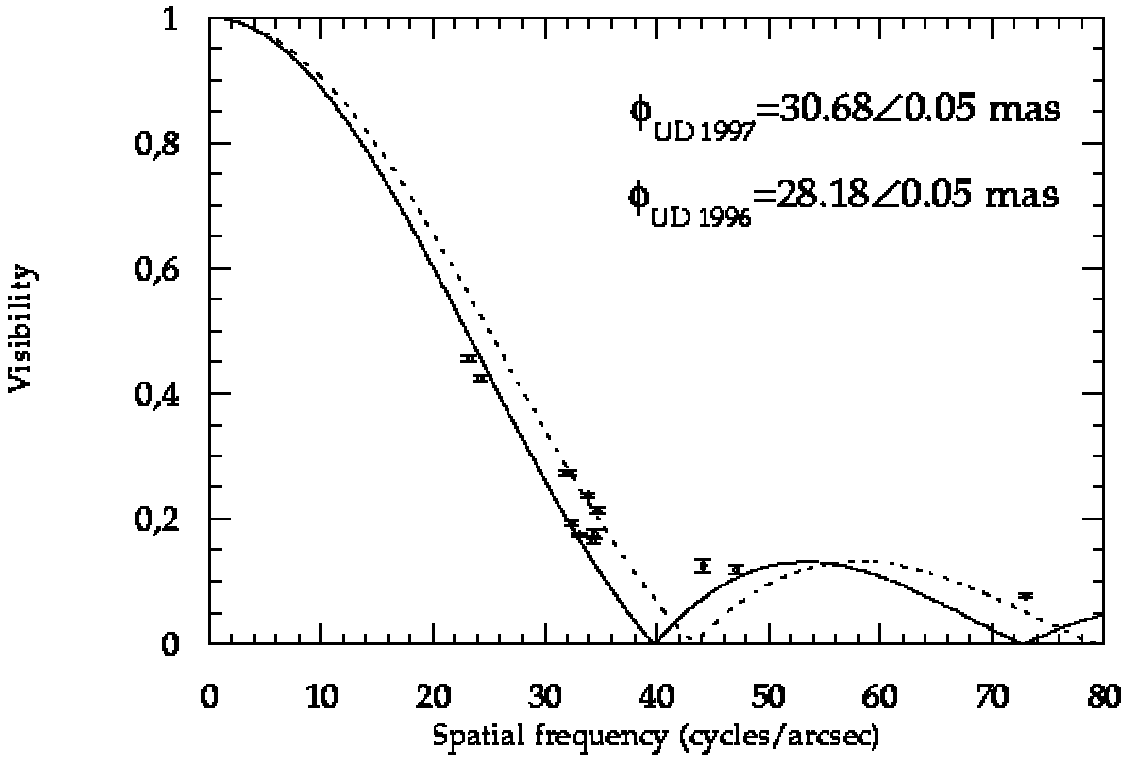


The first direct detection of the variation of the size of the photosphere of R Leonis from phase 0.24 to phase 0.28 generated by the pulsation of the star. Comparison with a uniform disk model yields a photospheric radius intermediate between that of fundamental and first overtone pulsators. High spatial frequency data acquired in 1997 display an excess of visibility interpreted as the possible signature of scattering by molecular species in the atmosphere. A direct effect of scattering on models is to yield lower values for the photospheric radius to 22 and 24 mas which make R Leonis a fundamental pulsator. Disagreement with dynamical models of Miras which predict that the diameter of the photosphere should decrease after phase 0.2.

# Cyclic variations in the angular diameter of Chi Cygni

J. S. Young et al., Volume 318 Issue 2 Page 381 - October 2000

Direct detection of cyclic diameter variations in the Mira variable Cygni. Interferometric observations made between 1997 July and1999 September, using the Cambridge Optical Aperture Synthesis Telescope (COAST) and the William Herschel Telescope (WHT), indicate periodic changes in the apparent angular diameter at a wavelength of 905 nm, with amplitude 45 per cent of the smallest value. The star appears largest at minimum light. Measurements made at a wavelength of 1.3 m over the same period suggest much smaller size changes. This behaviour is consistent with a model in which most of the apparent diameter variation at 905 nm is caused by a large increase in the opacity of the outer atmospheric layers (which is mostly owing to titanium oxide) near minimum light, rather than by physical motions of the photosphere.

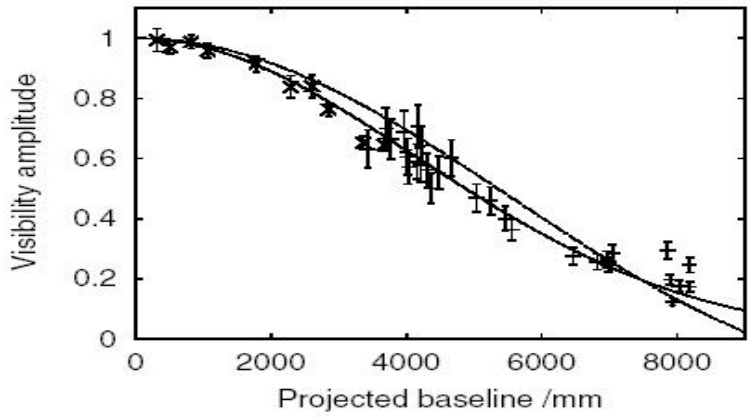


**Figure 1.** Visibility curve for $\chi$ Cygni at 905 nm. The vertical crosses are visibility amplitude measurements from COAST on 1997 August 7, and the diagonal crosses are averages of nine WHT measurements, at different baseline orientations, from 1997 August 11. The visual pulsation phase on these dates was 0.87. The best-fitting Gaussian (solid line) and uniform disc (dashed line) models are also shown. The Gaussian model is clearly a better fit to the data.

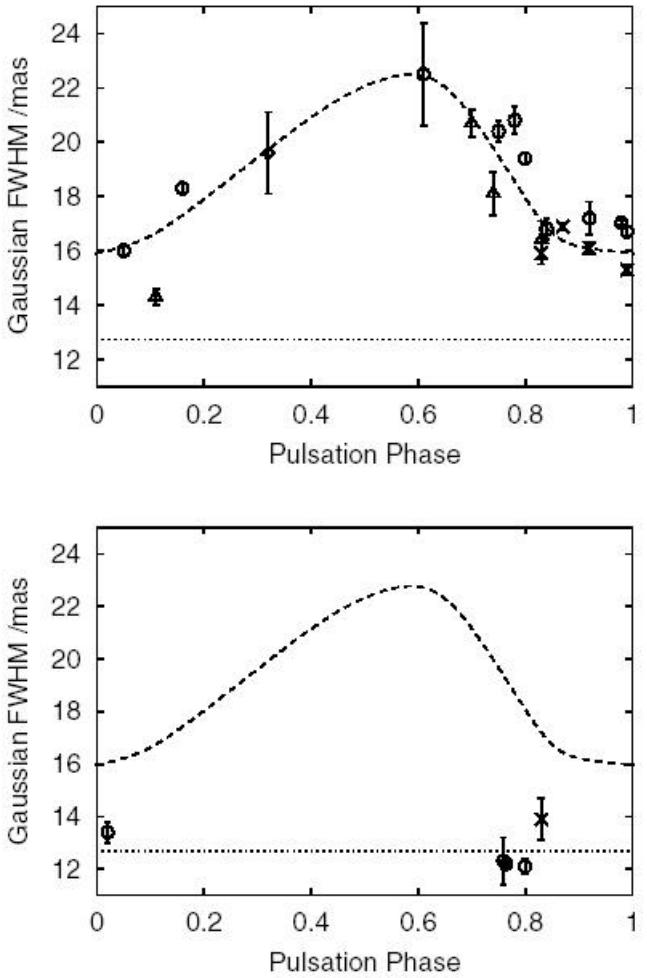


**Figure 2.** Apparent angular sizes (Gaussian FWHM intensity) and $1\sigma$ errors for $\chi$ Cygni at 905 (top) and 1290 nm (bottom), plotted against the phase of the visual light-curve (zero represents maximum visual light). Three consecutive cycles have been folded into a single plot: crosses indicate 1996–7 measurements, circles 1997–8 measurements, and triangles 1998–9 data. The diamond at phase 0.32 is the 1992 measurement at 902 nm of Haniff et al. (1995). The 905-nm diameter increases slowly from phase 0.0 to phase ~0.5, decreases rapidly between phases 0.6 and 0.8, then stays approximately constant up to maximum light. This generic variation is indicated by the dashed line, which is reproduced in the lower plot to highlight the very different behaviour at 1290 nm. A similar slow diameter increase during the first half of the pulsation cycle is seen in the B98 measurements of R Leonis. The dotted line (also superimposed on the 905-nm plot) roughly indicates the mean 1290-nm diameter.

## Precision Measurements of the Diameters of  Orionis and  Ceti at 11 Microns

Weiner et al., The Astrophysical Journal, 544:1097-1100, 2000 December 1

The angular diameters of  Orionis and  Ceti were measured at a wavelength of 11.15 microns using the two-telescope Infrared Spatial Interferometer (ISI). Fitting the visibility data to uniform disk models, the diameter of  Orionis is 54.7 ± 0.3 mas and that of  Ceti at phase 0.90 is 47.8 ± 0.5 mas. The effects of limb darkening and stellar hot spots are small at these wavelengths.

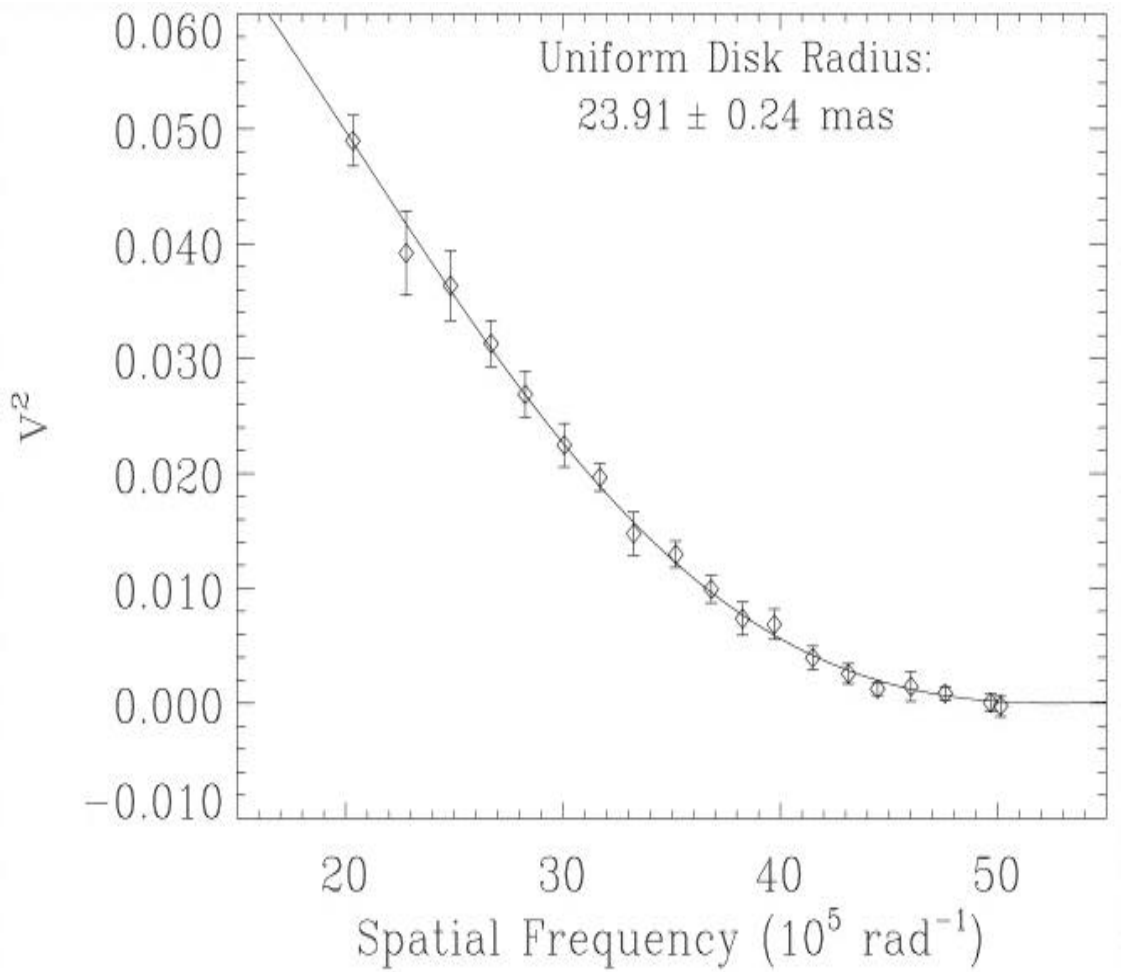

# The stellar atmosphere ?

Stellar sizes as a function of wavelengths give access to :

- Linear radii and effective temperatures
- Constraints to photospheric models. Not adequat apparently (molecular absorptions and diffusion), only simple interpretations are conveniently used.
- Pulsation modes (however non clearly identified); contribution between ratiative transfer in the atmospheric layers and true physical motion of the atmosphere (not yet well determined)
- Shock waves (not discussed here)
- Hot spots, asymmetries (not discussed at all here)
- …

In red are the important ingredients for understanding the rise of the wind producing the mass loss phenomenom

# The circumstellar medium ?

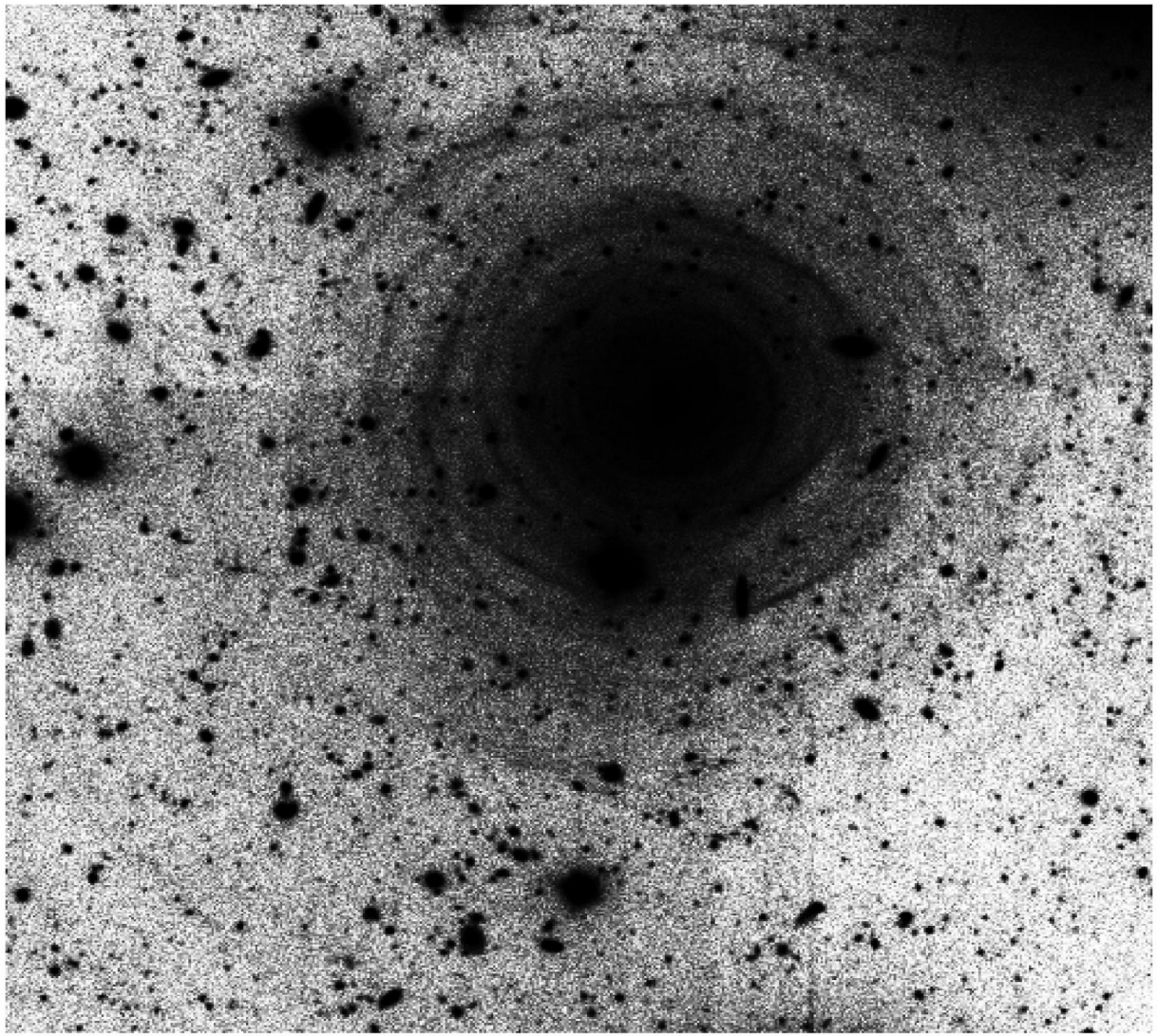

De Laverny et al., 1998 IAUS, 191

## « Photon » propagation

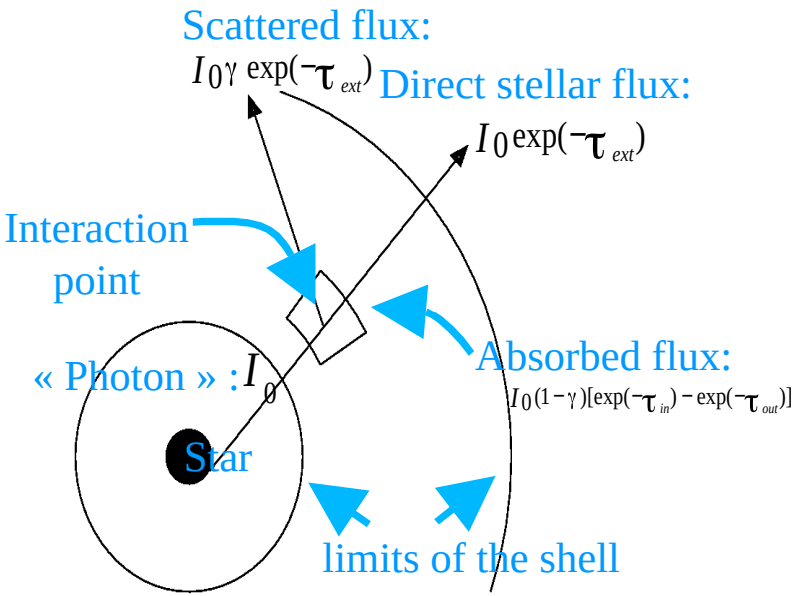

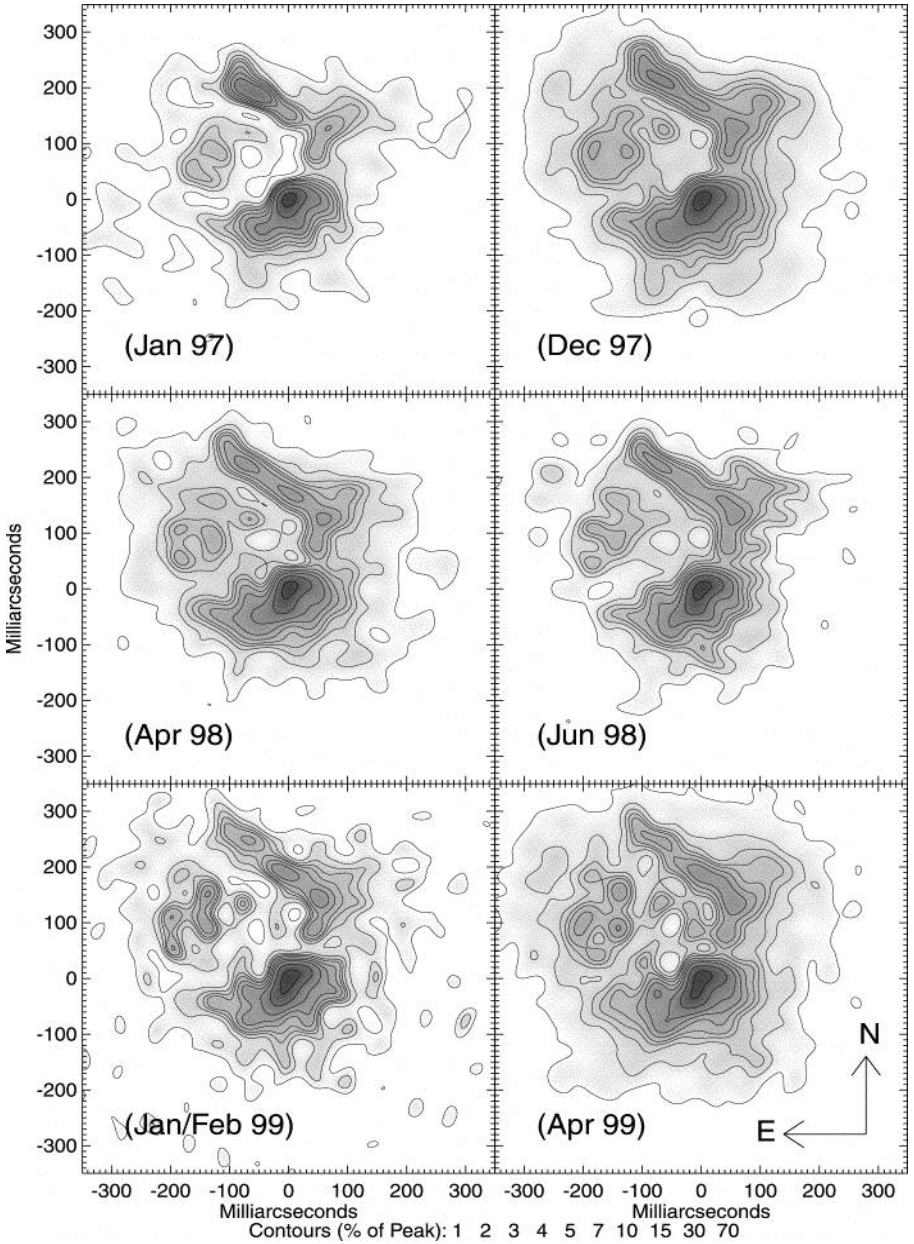


Smoke signals from IRC+10216 …

Tuthill et al., 2000, ApJ 543, 284

Osterbart et al., 2000,AA 357, 169

Some dynamical model in progress,

Col. with P. Woitke, G. Niccolini

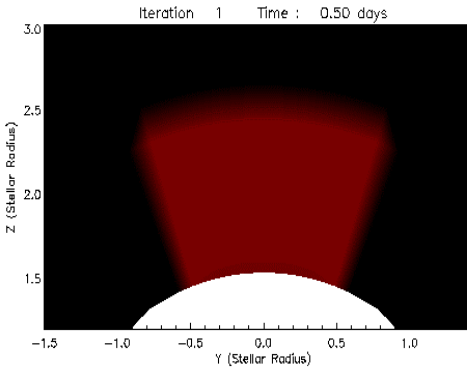


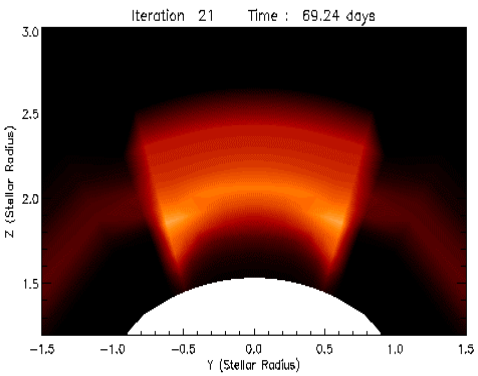

# Characteristics of dust shells around 13 late-type stars

Danchi et al., 1997, The Astronomical Journal, vol. 107, no. 4, p. 1469

The spatial distribution of dust around a sample of 13 well-known late-type stars has been studied with the Infrared Spatial Interferometer (ISI) located at Mount Wilson.

Dust production has stopped or has slowed in recent 3 years. Dust does not form every pulsational cycle (638 days).
Monnier et al., 2000, ApJ 543, 861.

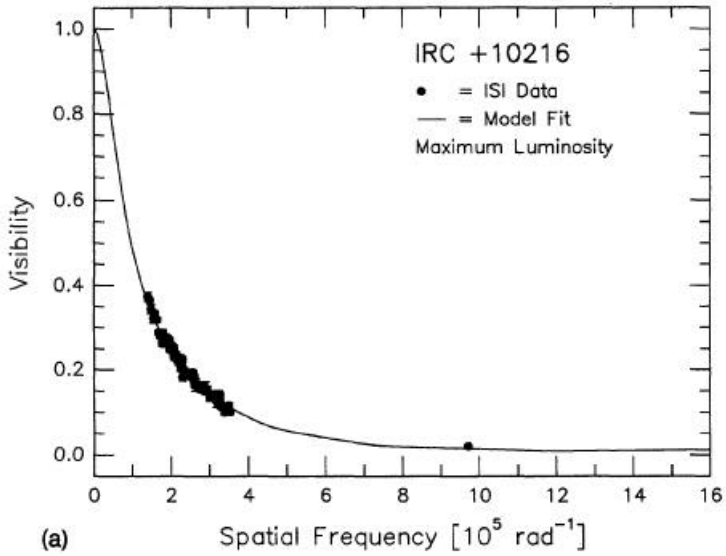


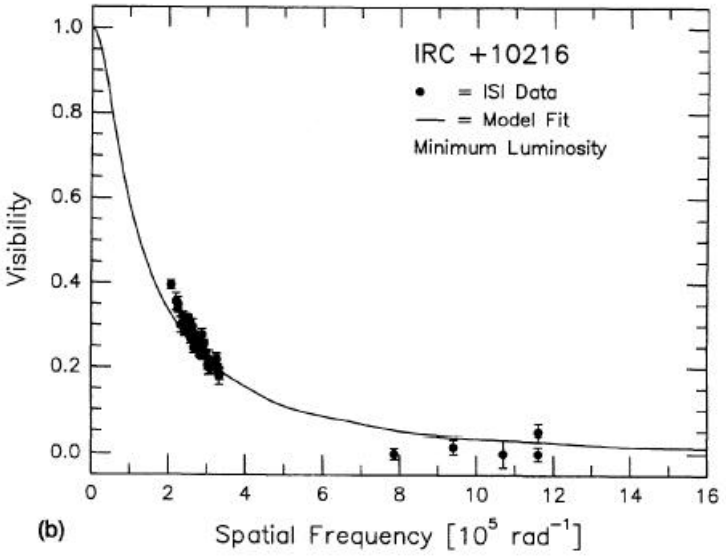


FIG. 1. IRC+10216 visibility data at maximum luminosity (a) and minimum luminosity (b) are given by the filled circles. Error bars reflect only the statistical uncertainty in the measurements. The solid lines represent best fit models described in Table 6 for (a) and (b), respectively.

Broadly speaking, two classes of stars have been found. One class has inner radii of their dust shells very close to the photospheres of the stars themselves (3-5 stellar radii) and at a higher temperature (approximately 1200 K) than previously measured.

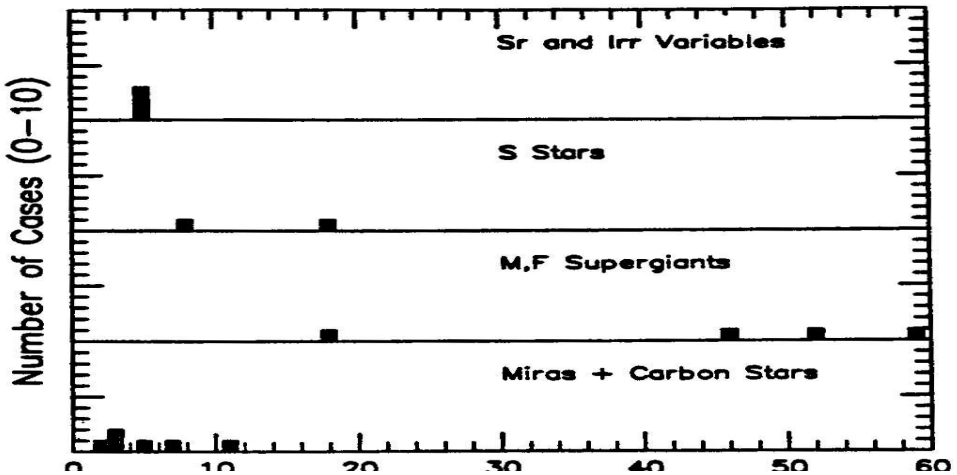

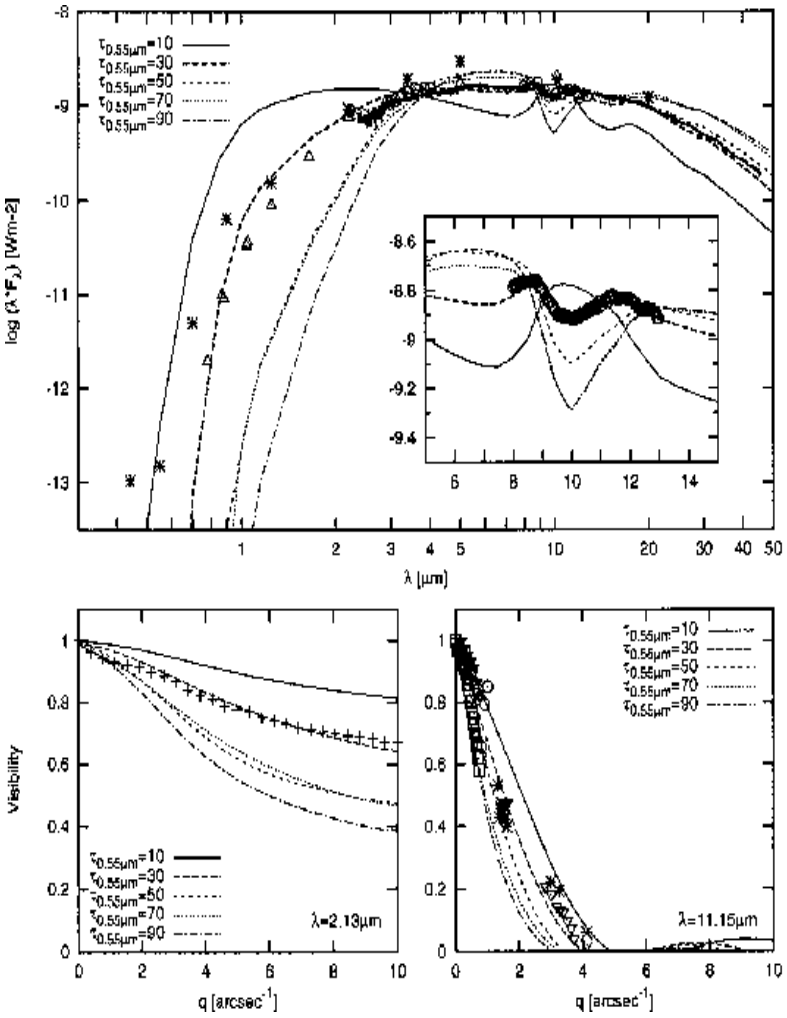


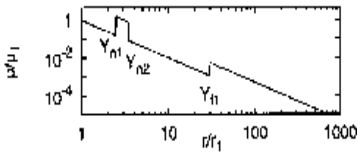


Bispectrum speckle interferometry observations and radiative transfer modelling of the red supergiant NML Cyg. Multiple dust-shell structures evidencing previous superwind phases.

Blocker et al., 2001, Astronomy and Astrophysics, v.369, p.142

Nonspherical Structures and Temporal Variations in the Dust Shell of O Ceti Observed with a Long Baseline Interferometer at 11 Microns

Lopez et al., 1997, Astrophysical Journal v.488, p.807

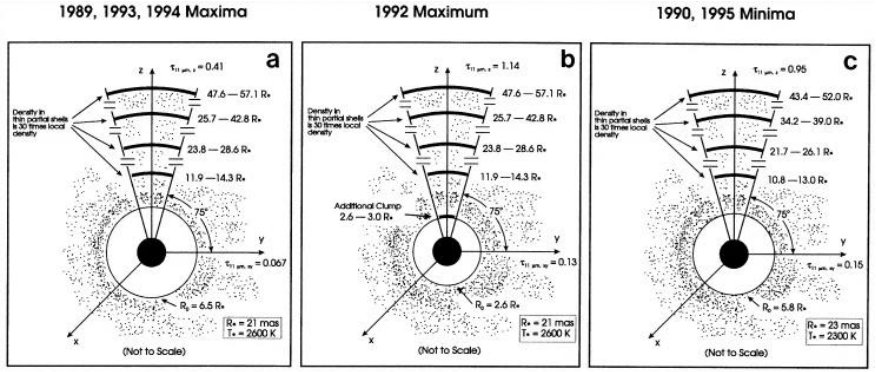


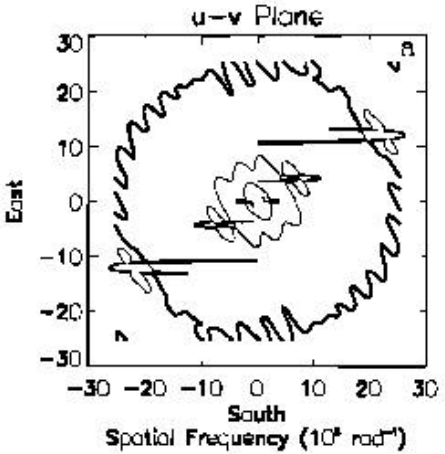


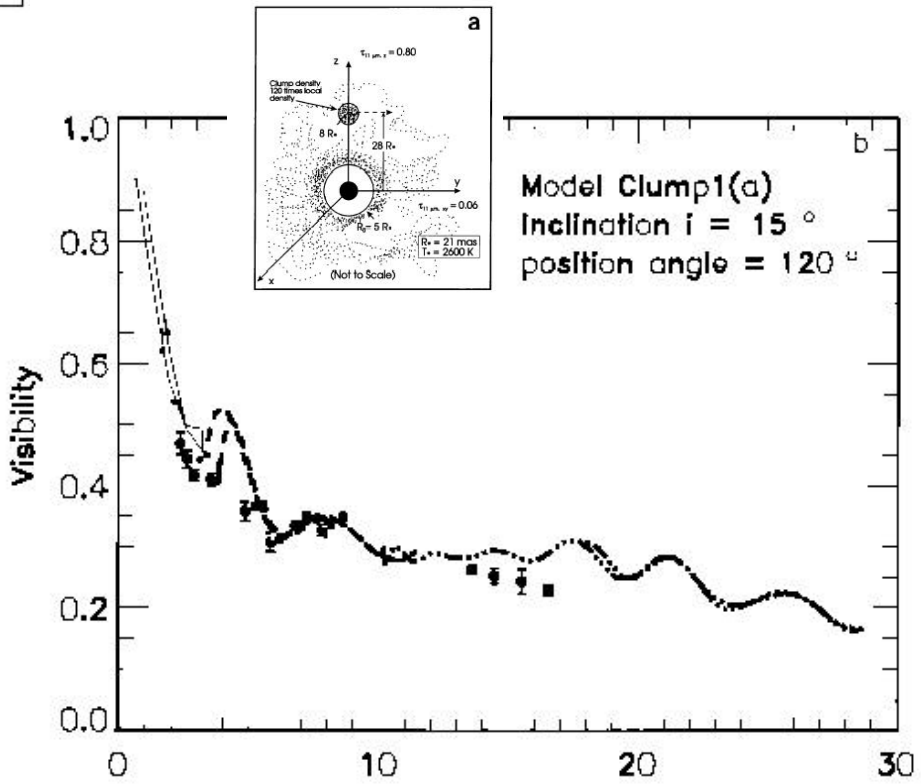

# Mass loss phenomenom in binary systems ?

## Omicron Ceti

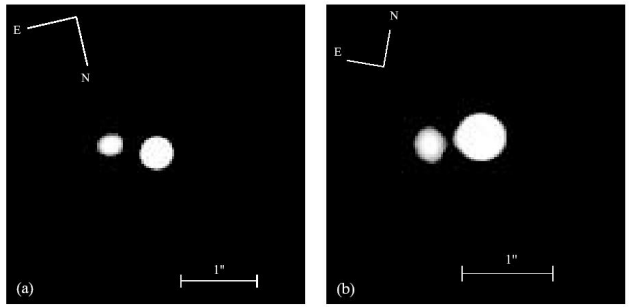


FIG. 1.—Restored images of Mira and its companion. (*a*) Mean of all *B* data from 1995 December 11, corrected by method 2 and restored using the iterative process described in § 4.2. (*b*) *V* data from 1998 August 29, corrected by method 2, and restored with bispectral method. For both images, the companion is on the left.

## Red Rectangle

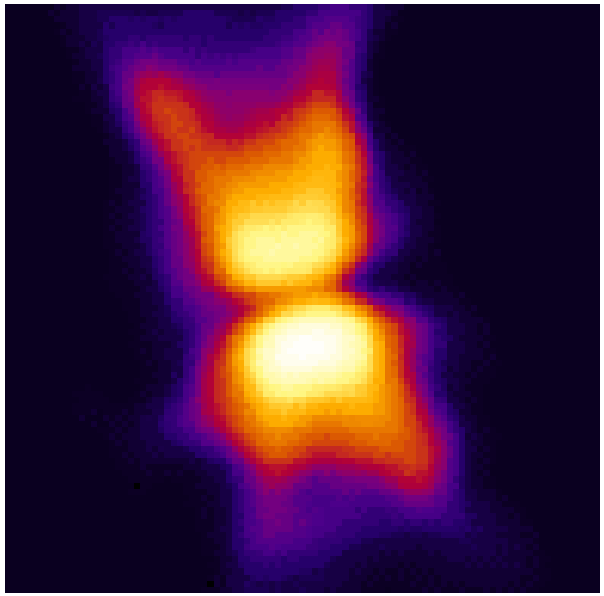

## Stingray Nebula

## WR 104 at 2.27 Microns

**April 98**

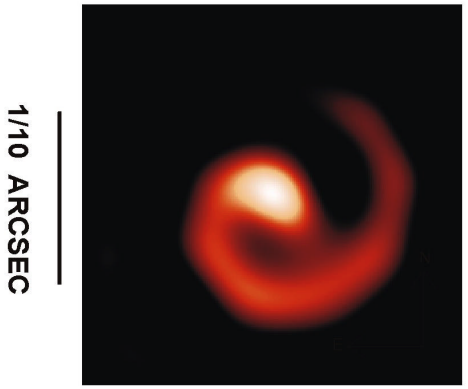


Interacting Binary Wind Model
of Spiral Outflow Around WR 104

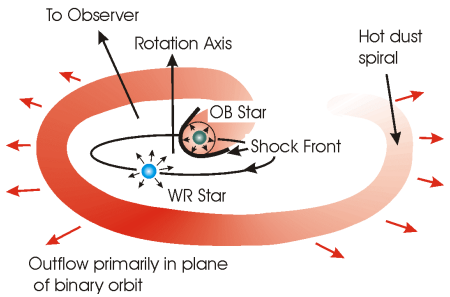

# The circumstellar medium ?

Its observations give access to :

- Optical depth, amount of dust and gas, recycled amount of material
- Typical size of regions where dust forms, dust characteristics
- Temporal evolution of dust formation and effects on mass loss
- Geometry of the wind : bipolarity, clumps at the star scale
- Mass loss events and link with the shock waves produced by the star
- Masers (not discussed here)
- Abondances in the wind
- …

In red are the important ingredients for understanding the dust driven wind